JET-R(95)10

Final Report for the ITER Contract"Deuterium Content of Material Redeposited in Tokamaks"

J P Coad

JET Joint Undertaking, Abingdon, Oxfordshire, OX14 3EA, UK.

This work was performed under NET Article 7 contract NET-94/870 in the context of the European Home Team contribution to ITER (ITER Task T61 of the 1994 Comprehensive Task Agreement)

December 1995

ABSTRACT

Methods have been assessed for the analysis of thick layers of redeposited material such as may occur in ITER, using a film ~100 μm thick from JET as a test sample. Neutron-induced Elastic Recoil Detection (n-ERDA) was found to be particularly useful. A comparison of the retention of D was made between the graphite and Be divertor tiles used in different phases of the 1994-1995 JET operations. The redeposited films were a mixture of C and Be in each case due to incorporation of material eroded from the main chamber. The overall rate of retention in the divertor was similar whichever tiles were used, and it was found that layers saturated with D were formed on cooled areas of tiles shadowed from the plasma. If surfaces are held at higher temperature (e.g. 300°C or above) the retained D concentration is an order of magnitude less. Diffusion effects were observed into the Be tiles which require further analysis.

1. INTRODUCTION

This Contract has covered two aspects of the generic topic "D content of material redeposited in tokamaks": how do you measure the D content of thick redeposited layers (>>10 microns), and how did the amounts of D compare in the graphite and beryllium tile phases of the 1994-5 JET campaign? The first part has been reported in depth in previous reports on the Contract and will not be discussed further here, but a paper which will be published in J Nuclear Materials describing the results is appended as Appendix A. The remainder of this report covers data from the JET operations of 1994-5 which used the new divertor and made a comparison between target tiles of two materials relevant to ITER - graphite and beryllium.

2. THE JET DIVERTOR

A new divertor structure, including four extra poloidal coils was installed in the bottom of the JET vessel in the period 1992-4. In the first phase of operations from April 1994 to March 1995 the divertor was fitted with graphite target tiles, and for the period April to June 1995 it was fitted with beryllium tiles. The support structure for the tiles is formed from 192 poloidal cooling pipes, each being covered by pairs of tiles clamped either side of the pipe, there being 19 pairs attached to each pipe (4 to form the inner divertor wall, 10 to form the floor and 5 the outer wall). A cross-section of the divertor along one of these support pipes is shown in Fig.1, and a more general view of a section of divertor in Fig.2. It can be seen in Fig. 2 that the tiles become narrower as the vessel radius decreases (from 40mm wide at the outer side of the divertor to ~30mm at the inner side), and that there is a gap between adjacent rows of tiles which remains roughly constant. The tiles were shaped so that each tile protects the edge of the next tile from direct impact from the plasma as shown in Fig.3, thus preventing the

"blooming" experienced in JET in previous campaigns: variations in the tile separations/vertical adjustment meant in practice that the size of "shadow" cast by one tile on the next alternated between ~50% and ~15% of the tile width.

The new divertor was fitted with target tiles made from 2-D carbon-fibre reinforced graphite, arranged with the weave planes normal to the plasma-facing surface, and operations commenced in April 1994. One poloidal set of tiles was removed for analysis (and replaced with similar tiles) at a vessel opening for repairs in September 1994. In March 1995 all the graphite divertor tiles were removed and replaced in the following month by beryllium tiles for an intensive two month campaign to compare the two target materials. In the last week of this campaign the power flux to the tiles was deliberately increased to levels at which surface melting of the Be tiles occurred. The melting was most severe on tile 12 (at the outer strike zone) where approximately two-thirds of the area exposed to the plasma had melted at some time and re-solidified, and about 1 mm of material from the surface in the centre of the tile was missing. Tile 8 (the inner strike point) had also melted and re-solidified over about one-quarter of the exposed area. Small melt areas were also visible on the adjacent exposed corners of tiles 10 and 11, resulting from incidents such as giant ELMS earlier in the Be tile campaign. Fig. 4 is a photograph of the tiles after operations and also shows that the tiles are castellated by cutting (to a depth of about 5 mm) the plasma-facing surface into areas about 8x8 mm to reduce thermal stresses. The plasma-exposed areas in the SOL appeared dark in the inter-shot viewing camera during the latter part of the campaign, and when the plasma was moved onto such areas there was invariably an increase in the optical emission from recycled D and Be.

3. ION BEAM ANALYSIS TECHNIQUES

The divertor tiles were analysed using a range of Ion Beam Analysis (IBA) techniques in a large chamber able to hold a number of samples the size of the divertor tiles at one time, and equipped to handle materials contaminated with beryllium. The elements D, Be and C can be analysed by Nuclear Reaction Analysis according to the reactions

$$^{2}D(^{3}He,p)^{4}He\ ,\ ^{9}Be(^{3}He,p)^{11}B\ \ ,\ ^{12}C(^{3}He,p)^{14}N$$

The three elements can be analysed simultaneously by using a ^{3}He ion beam and detecting the secondary protons produced at different energies by the reactions. However, the cross-sections for the reactions are very different in form, as can be seen in Figures 5 and 6 which show the variation in cross-section with primary ion beam energy for D and C, respectively. In order to measure C (and Be) it is necessary to employ a beam energy well above the threshold for the reaction of ~1.2 MeV - typically a 2.5 MeV ion beam is used.

Such a beam energy can equally well be used to detect D (though the greatest sensitivity occurs at an energy of 0.7 MeV), but it is important to consider the effect on the analysis of variations in the **depth** distribution of each element. As the ^{3}He ions travel further into the surface they progressively lose energy, on average at about 0.35 MeV per micron travelled, and at each point the cross-section varies accordingly. For C atoms encountered along the ion's path the cross-section drops sharply, so that the analysis is dominated by the C concentration in the first micron of material (ie. for normal incidence at a surface, the outermost micron of that sample). In fact, for a pure carbon sample such as clean graphite, NRA using a 2.5 MeV beam sees ~10^{19} C atoms, which means the combination of the cross-section and beam stopping functions gives a mean analysis depth of 1 micron. On the other hand, for D the cross-section actually **increases** with decreasing ^{3}He ion energy until the ion energy is reduced to ~0.5 MeV when the cross-section rapidly falls to zero. Thus D is detected to a depth of ~7-8 μm, with the sensitivity actually being greater deeper into the surface than it is in the outermost micron, for a normal incidence 2.5 MeV beam. Furthermore, because of momentum conservation effects, the emitted proton energy in the ^{2}D(^{3}He,p)^{4}He reaction varies with the ^{3}He ion energy. Fig.7 shows the proton peak observed from D atoms at a graphite surface for incident ion energies of 2.5, 1.2 and 0.5 MeV. The peak shifts by 47 channels over this range, which means that for a 2.5 MeV beam incident on a thick film containing D the resulting secondary proton feature can be deconvoluted to estimate how much of the feature results from reactions with different ion energies (and hence how much results from reactions at each depth, up to the maximum of 7-8 μm). Fig.8 shows an example of a proton peak from D that has been deconvoluted into several components which are then used to produce an approximate depth distribution for D in the surface. Note, incidentally, in Fig. 7 how the proton peaks characteristic of C disappear at the lower beam energies.

Other elements can be detected using other IBA techniques. Rutherford Backscattering Spectroscopy (RBS) detects incident particles scattered back from the surface, and their energy depends on the atomic mass of the scattering atom. Using a ^{4}He ion beam RBS is particularly suitable for detecting heavier impurities in a low-Z matrix such as we have in this work. If the impurity is localised at the surface, a peak appears in the spectrum corresponding to the elastic scattering of the α-particle, whilst a uniform concentration into the sample produces a step in the spectrum with the edge at the elastic scattering energy and a constant level to lower energy from particles scattered within the surface which lose energy both entering and leaving the surface. Fig.9 shows a spectrum from a relatively clean area of graphite divertor tile (upper part of figure), which is dominated by the edge for the C substrate, and from areas with a few % of Ni, Fe and Cr (the main constituents of inconel) and O in the outermost few microns (which gives a comensurate reduction in the C feature)(lower part of figure). RBS using ^{4}He is relatively insensitive for the light elements (a quite large Be level is hardly visible in Fig. 9), but using an incident proton beam gives very

good resolution for the light elements at the expense of mass number resolution for heavier impurities, as seen in Fig.10 which is from the same area as the lower part of Fig. 9.

Another method to detect any element with Z>8 is Particle Induced X-ray Emission (PIXE). An incident ion beam excites core electron binding levels in atoms present in the surface region, each of which de-excites by an electron dropping down from an outer shell. The energy difference between the levels given up by such an electron is emitted as an X-ray which is thus characteristic of the particular element, and the X-ray energy spectrum can therefore be used to analyse the surface (the information coming from the outermost 5 microns, approximately). Fig.11 gives the PIXE spectrum for the area in Fig. 10, recorded simultaneously using the same primary beam.

4. D AND IMPURITY ANALYSIS OF THE GRAPHITE TILES

An overall view of the D distribution on the divertor floor tiles removed from the torus in September 1994 is shown in Fig.12 (for the outer half of the divertor), and in Fig.13 (for the innermost pair of floor tiles). For the tiles within the scrape-off layer (SOL) for most discharges (tiles 5 to 7 and 12 to 14), the areas along the tile edges shadowed by the adjacent tile were obvious from the visual appearance of the tiles, being covered by a darker, less reflective layer. The areas shadowed by the inner and outer wall tiles on the ends of tiles 5 and 14, respectively were similarly marked. It is clear that the amount of D present in these shadowed areas is greater than in the regions exposed to the plasma, going through a maximum just within the shadowed region, as is seen in Fig.14, which shows the D, Be and C levels detected across tile 13A. (The data from two adjacent scans are superimposed.)

The most striking feature of the analyses of these tiles is the large concentration of D seen in the shadowed regions - up to 8.5×10^{19} atoms cm^{-2} in the shadowed region of the innermost floor tile, where a thick film with some localised spalling was visible. (On these tiles the deposition also continues all the way down the sides of the tiles, as evidenced by interference colours, indicating transport of impurities several centimetres down the gaps between tiles.) This D is clearly present in a film of greater thickness than the ~8μm analysis depth, so correcting for the varying cross-section with depth as discussed in the section above, this maximum concentration of D found on the tiles is approximately $5\text{-}6 \times 10^{22}$ cm^{-3} within the film, which gives a D:(C+Be) ratio of ~0.5:1. This ratio is similar to the saturation concentration of D in graphite found for surfaces implanted with D ions (1), and for C layers formed from methane by coating in a glow discharge (2).

In areas of tile exposed to the plasma the amount of D retained near the surface is relatively low, typically 5×10^{17} atoms cm^{-2}. However, there are no areas with very low levels such as occurred at the strike points on the upper X-point tiles after operations from June 1991 to February 1992 (~10^{16} and ~4×10^{16} cm^{-2} at the outer and inner strike zones, respectively

(3)). This may be because during most discharges in the 1994-5 campaign the strike points were each swept at 2 Hz over a radial distance of several centimetres of divertor floor, which together with the larger contact area in 1994-5 meant the surface temperatures of the tiles were much lower than for an equivalent plasma power in 1991-2. It should also be recalled that the support bars are water-cooled, so that the starting temperature before a pulse is ~50°C and the tile surface returns to this temperature within a few minutes, whilst for the X-point tiles the base temperature was 250-300°C (the vessel temperature) and the tiles must lose excess heat primarily by radiation.

Shadowed regions close to the areas of greatest erosion (the strike zones) also existed on the upper X-points and were likewise covered with redeposited films with thicknesses which sometimes exceeded the NRA analysis range. However, the greatest D content in these previous deposits was an order of magnitude less than the maximum observed from shadowed regions on the 1994-5 divertor tiles. On the assumptions that the analysis depth was ~1 μm and perhaps half the H isotope content was present as ^{1}H, it was assumed that the 1991-2 deposits reached the saturation level for ($^{2}D+^{1}H$) in C of 0.4. However, the detailed analysis of the NRA data in section 3 above neccessitated by the 1994-5 results reveals that the D:C ratio in thick films previously observed in JET was never more than ~0.05:1 (ie. 5%). It is believed that the factor that makes the difference is the water-cooling of the JET divertor. The base level for the bulk temperature of the divertor tiles was 50° C, and during pulses the maximum bulk temperature for any tile was ~200° C (at the strike points). Although the surface temperature in regions exposed to the plasma would have reached much higher values, it may be assumed that the surface temperature in the shadowed region would not exceed the bulk temperature as thermal conductivity parallel to the surface is much less than normal to the surface for this 2-D weave orientation.

Tiles that were invariably within the private flux region (ie. tiles 9 and 10) retained low levels of D (~$5x10^{17}$ cm^{-2}) at all points, whether within or outside the shadowed area.

Fig. 14 showed a level of Be across the plasma-exposed surface of ~$1\text{-}2x10^{18}$ cm^{-2}, and this was typical of the Be level over all the areas in the plasma SOL. In the private region the Be level was an order of magnitude lower, and as seen in Fig.14 there was a sharp decrease in Be (along with the D) into the shadowed region. The principal source of Be in the machine was the regular Be evaporations from four equispaced heads at the outer midplane - although the RF antennae screens were also made of Be little use was made of them in the early part of the 1994-5 operations due to complications with the power supplies. However, the Be seen on the divertor tiles cannot come directly from the evaporations, since there is a poor line-of-sight from the divertor to the evaporators, so very little deposition would be expected. Furthermore, what deposition that did occur would be approximately uniform over all the tile surfaces. The Be must therefore be eroded from the walls of the main discharge chamber and transported along the SOL into the divertor, hence being deposited with the observed

distribution. (Since the PFC's of the main chamber are graphite, and the evaporation does not provide a complete cover, there must also be rather more C being deposited on the divertor, but this cannot be distinguished from the substrate carbon.) The levels in the shadowed areas and the private region reflect the low probability of deposition from the plasma in these areas. Note, however that unlike the D there is no significant peak of Be just into the shadow. This suggests that the film in this area is formed by carbon eroded from the divertor and redeposited locally (and saturated with codeposited D) and that the Be is not re-eroded with the same probability as C.

The areas with the largest amounts of deposited Be also bear the largest amounts of other impurities such as the elements that comprise inconel (Ni, Fe and Cr) as seen in Fig. 9 (lower part). These impurities were probably deposited during periods of operation when the plasma was in contact with unprotected parts of the vessel such as the upper saddle field coil housing (the repair of which neccessitated the vessel opening during which these tiles were removed).

A complete poloidal set of graphite tiles removed in March 1995 have also been analysed, confirming the pattern of D retention on the floor tiles. Increased levels of Be were found on tiles 7 and 12 (~5×10^{18} cm^{-2}), ie. in the areas where deposition from the plasma might be expected to be greatest. There was also deposition containing D, Be and other impurities on the inner wall tiles similar to that on floor tiles in the inner SOL, with, for example, codeposited D in the shadowed region of tile 2 also at the saturation level for films >8 μm thick. In contrast, however, the outer wall tiles appeared much cleaner than either the floor or inner wall tiles, with little evidence of redeposited films. A similar effect occurred with the upper X-point tiles in 1990-2, in that beyond the outer strike-point region the tiles were quite clean whereas there was heavy deposition around the inner strike zone (3).

5. D AND IMPURITY ANALYSIS OF THE BERYLLIUM TILES

The analysis of the Be divertor tiles that were in use from April to June 1995 is incomplete, but several tiles have been analysed and the general picture is fairly clear. Firstly, the amount and distribution of D retained on the Be tiles is similar to the results described above for the graphite tiles. High concentrations of D are retained in deposits in the shadow areas (which are similar in size to those on the other tiles) and thick films are clearly visible at the inner corner of the divertor. An NRA spectrum from a point in the shadow region on tile 6B (at the end deepest into the SOL) with a D signal of 2×10^{19} cm^{-2} is shown in Fig.15(a), whilst the spectrum shown previously in Fig.8 was recorded a few millimetres away on the plasma-exposed part of the same tile (which appear dark in Fig. 4 as mentioned in Section 2) and has a D level of ~6×10^{18} cm^{-2}. Fig. 15(b) comes from the other end of tile 6B (the plasma-exposed area nearer the strike point) and has a D level of ~1.5×10^{18} cm^{-2}.

The spectra in Figs.8 and 15 contain a number points of interest. Firstly, the large D feature from the shadowed area is strongly peaked near the surface, so that although the amount is about one-third that from a corresponding area on a graphite tile, the D concentration in the outermost micron is similar in each case, but the layer is thinner. Secondly, the D peaks from the plasma-exposed regions though smaller are broader, indicating that the D is present for several microns into the surface at lower concentrations of ~0.08 and ~0.02 times (Be+C). Finally, the spectra from the plasma-exposed areas contain small peaks characteristic of C (though these represent 3-4x10^{18} cm^{-2} since the sensitivity is less than for D or Be), whereas C is greater in the shadowed area (in comparison to Be). On tiles 5A and 5B where the thickest films are found, these films are again saturated with D to >8 μm. In these areas the C:Be ratio is further increased, so that the outermost microns are mostly C (plus D).

In the centre of the melt region of tile 12B (where ~1 mm has been lost from the surface during the controlled melt experiment) the D was at a very low level (~1.5x10^{17} cm^{-2}), though there was a small C peak still visible. No spectra from Be samples have been recorded with smaller C features than this (eg. a similar level is found on the back of the tile), so it may be that a few times 10^{18} cm^{-2} of C comes from atmospheric exposure, handling and packaging during transport. The ^{1}H RBS spectrum from this area is shown in Fig.16(a). The spectrum may be taken as a reference spectrum for Be, though there are small peaks visible from near-surface traces of O, C and D.

The melted (and re-solidified) areas of tiles 12 and 8 have experienced surface temperatures of >1300°C (the melting point for Be) on occasions. Clearly the areas adjacent to such regions must also have been very hot at such times. It would be reasonable, therefore, to expect any retained D to have outgassed during the melting experiment, in the way it appears to have done from the thick C films on the 1986 limiters (see Appendix A). However, this does not appear to be the case. Fig.17 shows the NRA and ^{1}H RBS spectra from an area close to the melt region on tile 8A. The C appears in the NRA spectrum at its minimal value, and cannot be seen in the RBS spectrum, but there is quite a large D feature indicating D at a low level in the outermost 1-2 μm but then at ~10% through the remainder of the analysable depth (ie. to >8μm).

NRA is not ideal for analysing the C on these Be tiles due to the limited analysis depth. However, further information on the relative composition of C and Be is provided by ^{1}H RBS spectra, such as in Figs.16 and 17. Figs. 16(b), (c) and (d) come from tiles 5B (the plasma-exposed area deep in the SOL, so the corresponding NRA spectrum might be similar to Fig. 8), 6B (the shadowed area, close to the area from which the NRA spectrum in Fig 15(a) was recorded) and 5B (the area covered by a thick film), respectively. The spectra (all recorded with similar sensitivity) show increasing replacement of Be in the near-surface layers by C (and D). At the very surface, however, according to spectra (b) and (c) there is still a high Be

concentration which decreases into the C-rich band, whilst in (c) a small Be peak is sitting on top of a band of almost pure C+D.

The C must arrive on the divertor tiles via the plasma, having been eroded from PFC's in the main chamber together with some Be (as explained in the previous section to be the origin of the Be on the graphite tiles). An experimental confirmation of this mechanism is that even when the Be divertor tiles are the contact points, the C impurity level in the plasma is at least as large as that of Be for most discharges (4). The C must be deposited initially therefore in the plasma-exposed regions, however this is not where it is found. Local recycling occurs at the divertor surface, and this mechanism leads to a probability of redeposition in shadowed areas, which act as sinks. The films built up in these areas are predominantly C, yet the surface composition in the plasma-exposed areas is mostly Be, which seems to imply that chemical sputtering of carbon plays an important role in the local recycling process (as was implied in section 4 by the absence of Be in the deposits on graphite tiles). The layer appearing black on the surface of tiles in the SOL may thus be a honeycomb of Be from which C has been chemically etched and which may act as a conduit for D diffusion into the Be. Poor thermal conductivity through this layer may explain why there is a release of gas from these areas when they experience a plasma power loading.

This model can clearly account for the observed progressive accumulation of carbon in the shadowed regions. However, one might expect the C to form a layer on the surface, whereas the RBS profiles look as if the Be diffuses through the arriving C to the surface. Whilst this might be reasonable on the plasma-exposed area of tile 5 where there is frequent ion bombardment and occasional plasma heating (Fig 16(b)), it is unexpected in a normally cold shadowed area such as analysed in Fig 16(c). The apparant interactions on these divertor tiles between C and Be is an area for further study of obvious importance to ITER.

6. CONCLUSIONS

Methods of analysing thick films (i.e. 100's of microns) of redeposited material have been developed and applied to ~100 μm films from JET. Totally misleading estimates of the total H-isotope content of the films may be obtained if only the outermost few microns of the film are analysed. For example, the analysis of ~100 μm films from the flanks of a graphite discrete limiter used in JET during 1986 showed ~5% D in the outermost micron, but at least on order of magnitude lower concentration throughout the rest of the film.

The best technique for analysing H, D and T simultaneously in thick films was found to be Neutron-induced Elastic Recoil Detection (n-ERDA), which is also non-destructive if samples are less than a few millimetres thick. It is recommended that a dedicated n-ERDA system be set up for the analysis of films relevant to ITER.

Divertor tiles used in the 1994-5 JET campaign have been analysed. The patterns of redeposition, and the amounts of D retained in the JET divertor are similar for operations with graphite tiles and with Be tiles (though some Be tiles have still to be analysed before the total inventory can be compared with that on the graphite tiles).

Be is deposited on the graphite tiles, and C on the Be tiles, due to erosion from the walls surrounding the main plasma volume and transport in the SOL down into the divertor. (The impurities in the plasma seem to arise principally from this erosion, and not from the divertor target.) For each type of tile the composition of the D-containing deposits on the divertor is thus a mixture of C and Be.

In areas of tile shadowed from the plasma by adjacent tiles, where the base temperature was 50°C and the maximum temperature excursion (for a few seconds during plasma pulses) was 200°C, the ratio of D:(C+Be) reached ~0.5:1, through redeposited films >8 μm thick in some places (~5×10^{22} D atoms cm^{-3}). The amounts of D are an order of magnitude greater than ever found in JET prior to installation of the water-cooled divertor, even though those earlier JET surfaces were a similar mixture of C and Be: reassessment of previous analysis data shows that with a hot vessel (minimum PFC temperature of ~300°C) the maximum concentration through thick films was probably ~0.05:1. Further analysis of the depth distributions of retained D in these divertor tiles and previous JET samples is required.

On the areas of graphite tiles exposed to the plasma the D concentration is relatively low, ~5×10^{17} atoms cm^{-2} near the strike points rising to a few times 10^{18} cm^{-2} deeper into the SOL: such levels do not make an appreciable contribution to the overall inventory. Comparable levels are seen in the outermost few microns of the Be tiles. However, there is evidence of diffusion of D into the Be surfaces to >8μm at significant concentrations (~10%) even though the tile surfaces reached high temperatures during plasma exposure (areas of some tiles were deliberately melted as part of the Be tile assessment programme). The extent of this diffusion into the bulk requires further investigation, since it may have an important bearing on the retained H-isotope inventory if Be is used in ITER.

REFERENCES

(1) K L Wilson and W L Hsu, J Nucl. Mater.145-147 (1987) 727

(2) J Winter, ibid, p131

(3) J P Coad and B Farmery, Vacuum **45** (1994) 435

(4) The JET Team (presented by G F Matthews), 22nd EPS Conf. on Controlled Fusion and Plasma Physics, Bournemouth, UK, July 1995.

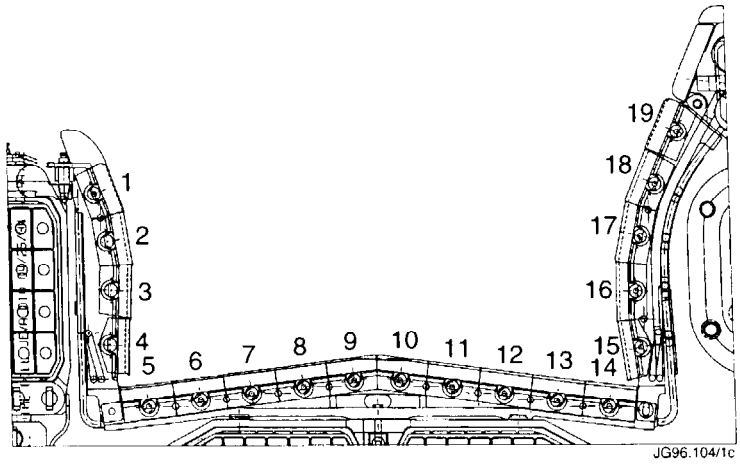

Fig.1: A radial cross-section of the JET Mark I divertor which was in use during 1994 and 1995.

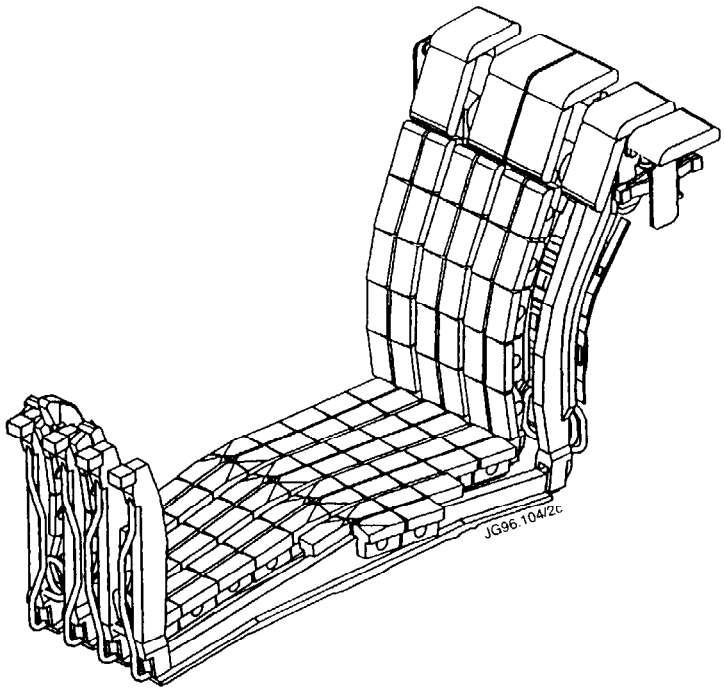

Fig.2: A drawing of a section of the JET Mark I divertor.

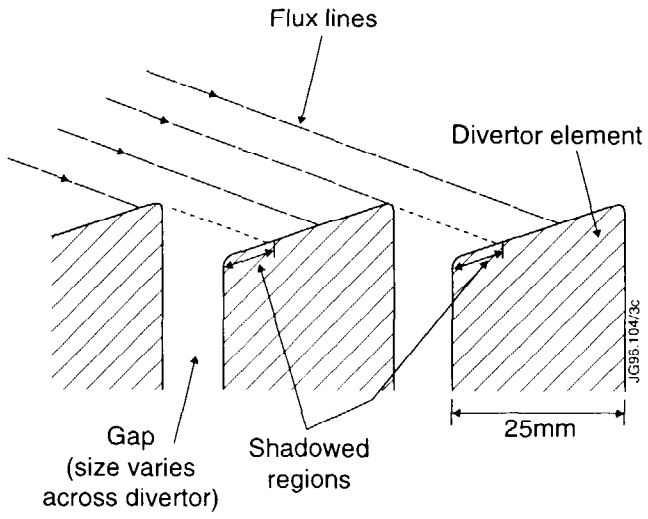

Fig.3: A schematic toroidal cross-section of some divertor tiles to show the shadowing of part of each tile by its neighbour

Fig.4:

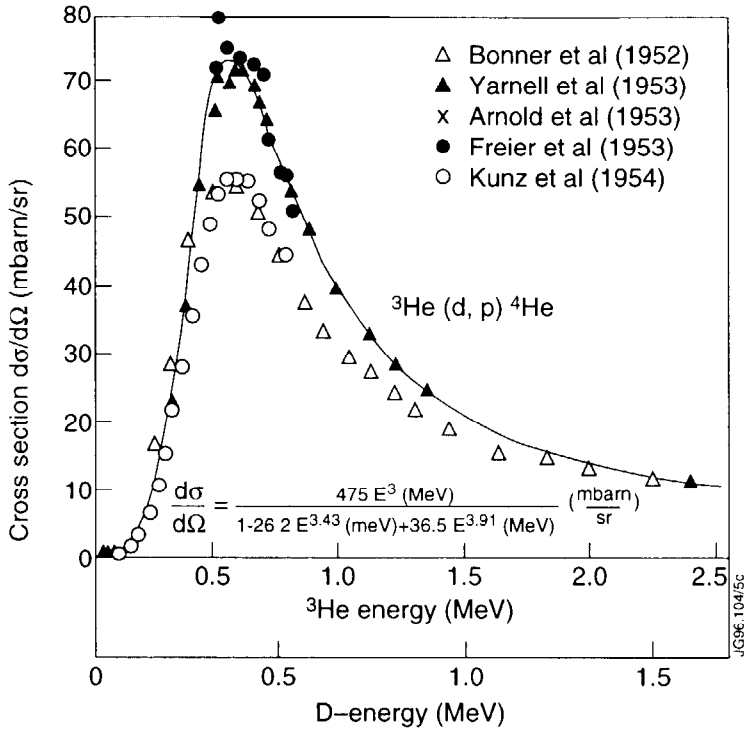

Fig.5: Differential cross-section for the ^{3}He (d,p)^{4}He reaction as measured by different authors.

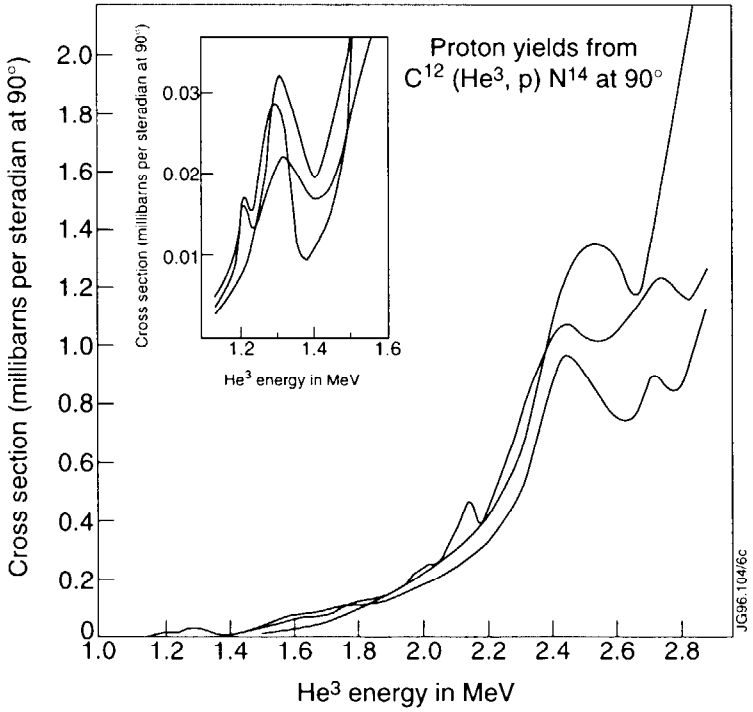

Fig.6: Excitation curves for protons from ^{12}C (^{3}He,p)^{14}N corresponding to formation of ^{14}N in its ground state and first two excited states.

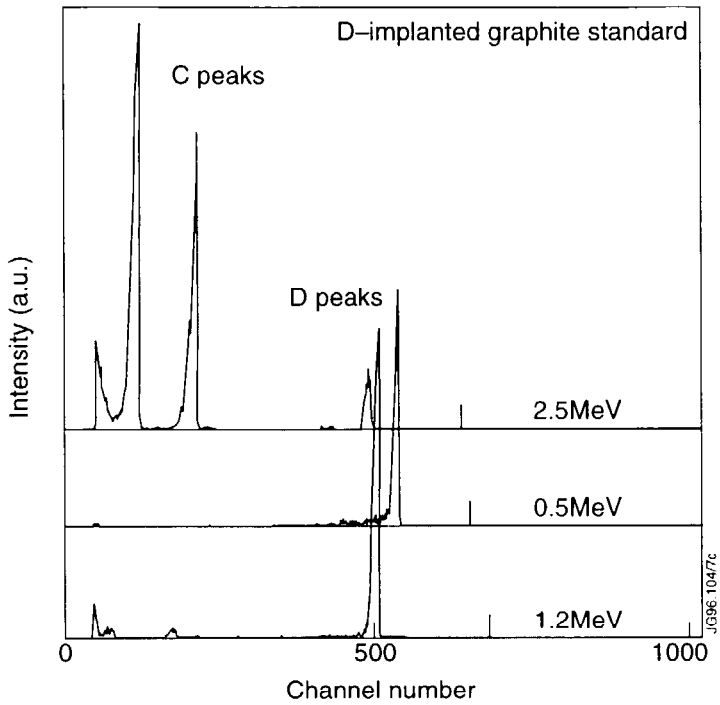

Fig.7: NRA spectra from a D-implanted graphite standard using three different ^{3}He primary ion beam energies.

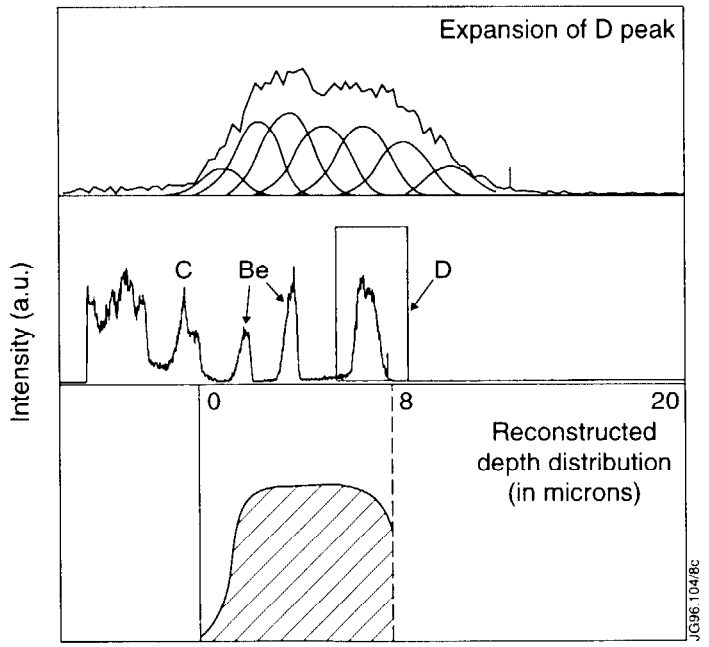

Fig.8: An NRA spectrum recorded with a 2.5MeV ^{3}He ion beam from a Be divertor tile exposed in JET in 1995 (central part of figure), with an expansion of the D peak (top part) and a reconstructed depth distribution using the data of Fig.6 and the stopping power for ^{3}He ions.

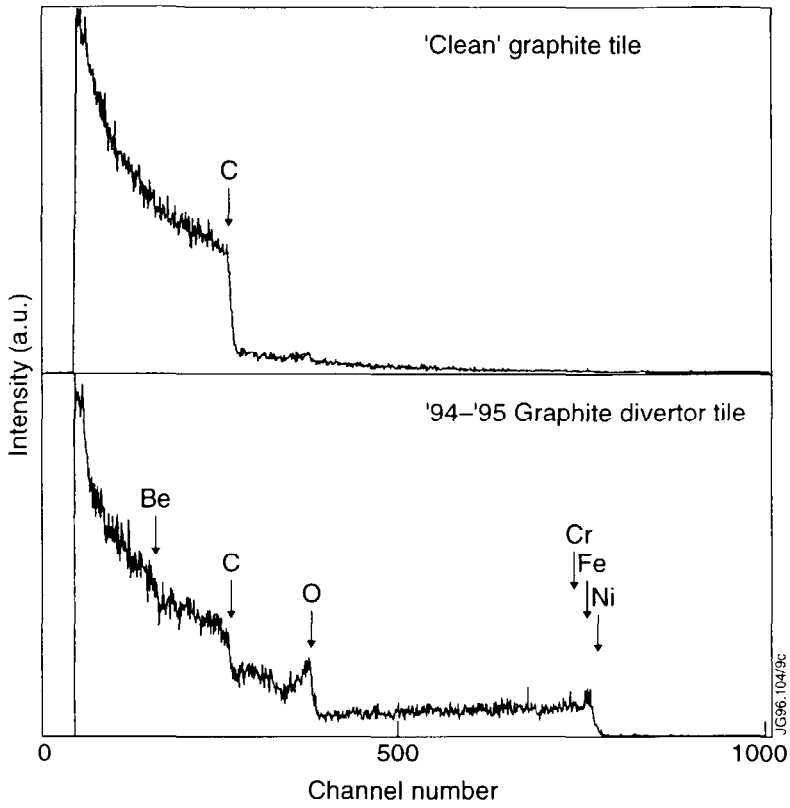

Fig.9: ^{4}He RBS spectra from a relatively clean area of the graphite divertor tiles (upper part), and from a tile showing heavy redeposition from the plasma (lower part).

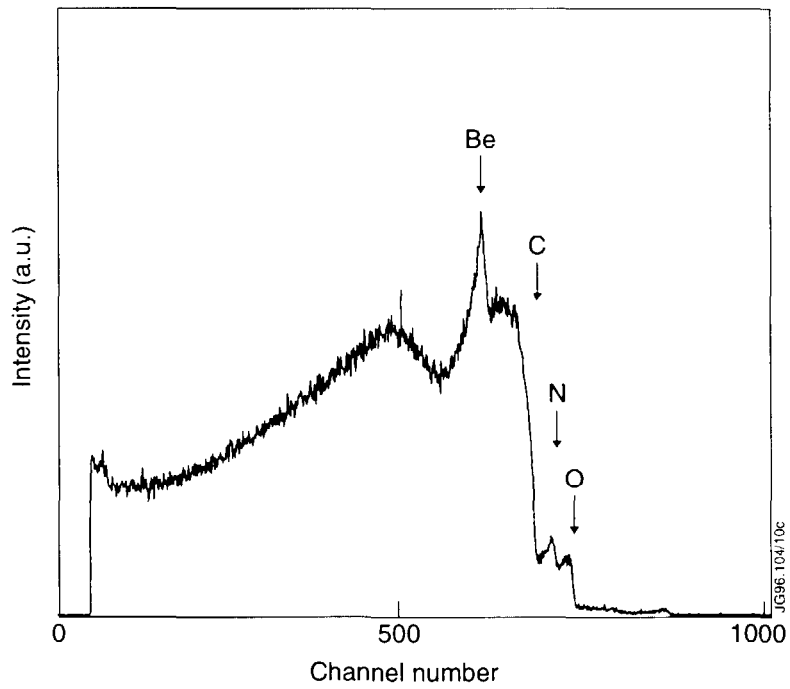

Fig.10: An RBS spectrum recorded using a proton beam from the same area as analysed in the lower part of Fig.9.

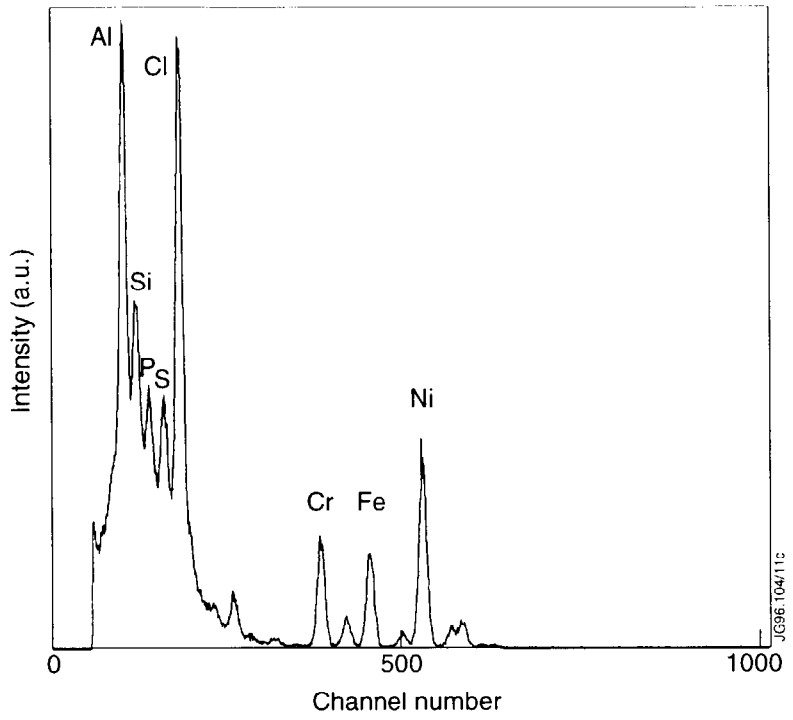

Fig.11: A PIXE spectrum recorded from the same area as the RBS spectrum of Fig.10 and simultaneously using the same proton beam.

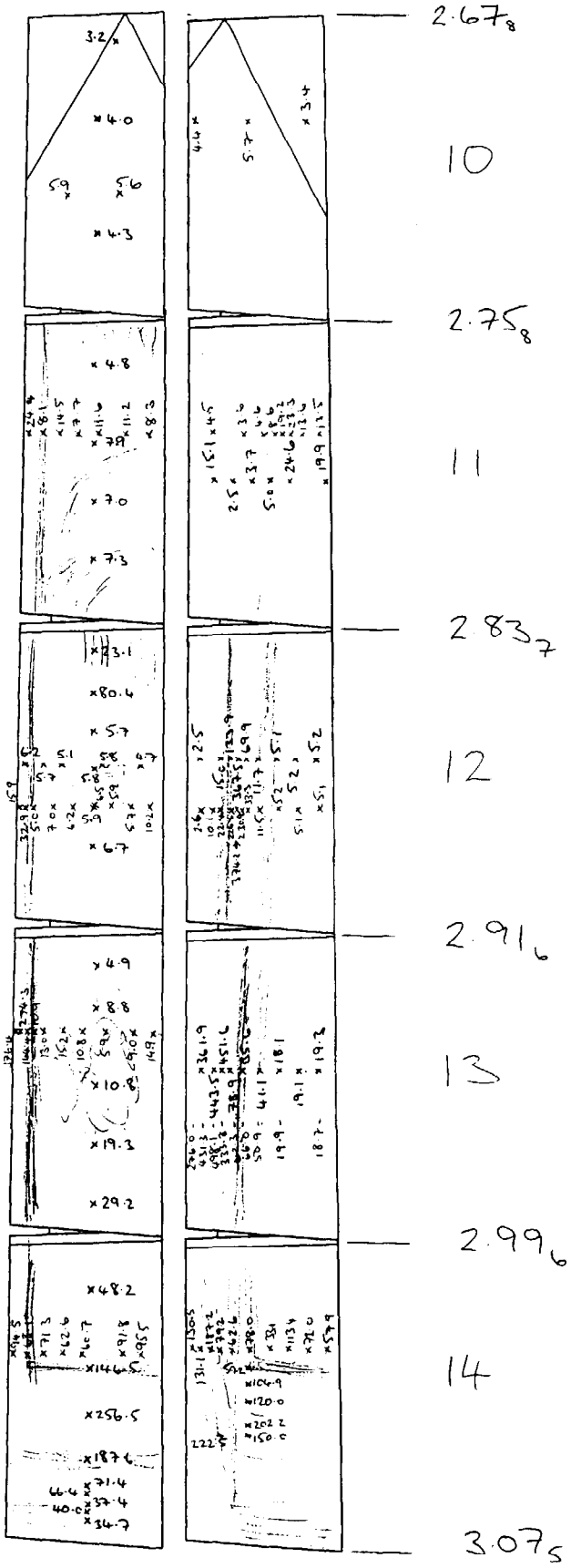

Fig.12: An overall view of the D distribution on the divertor floor tiles removed from the torus in September 1994 (for the outer half of the divertor), the D analyses being in units of 10^{17} atoms cm^{-2}.

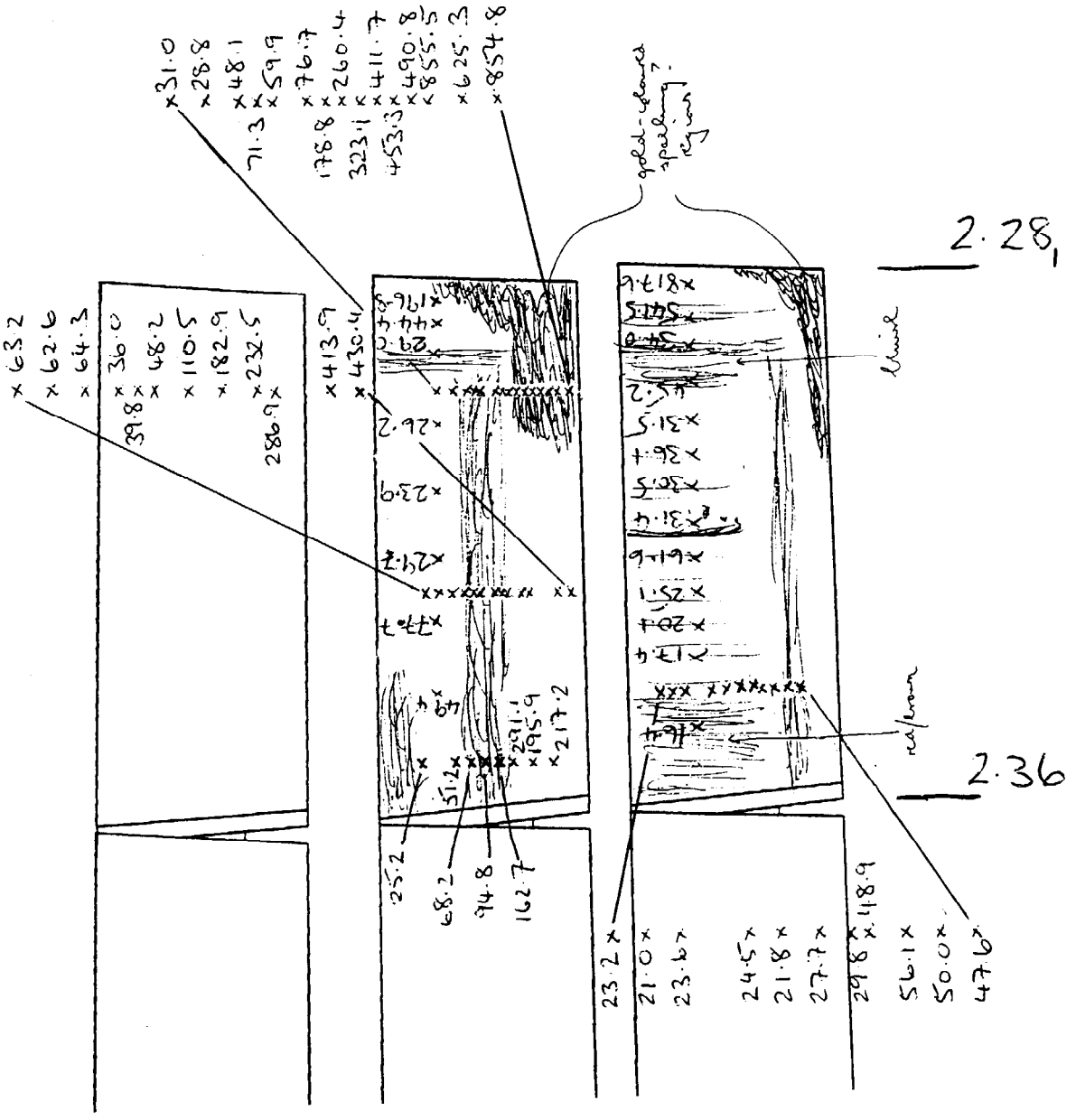

Fig.13: An overall view of the D distribution on the divertor floor tiles removed from the torus in September 1994 (the innermost two tiles), the D analyses being in units of 10^{17} atoms cm^{-2}.

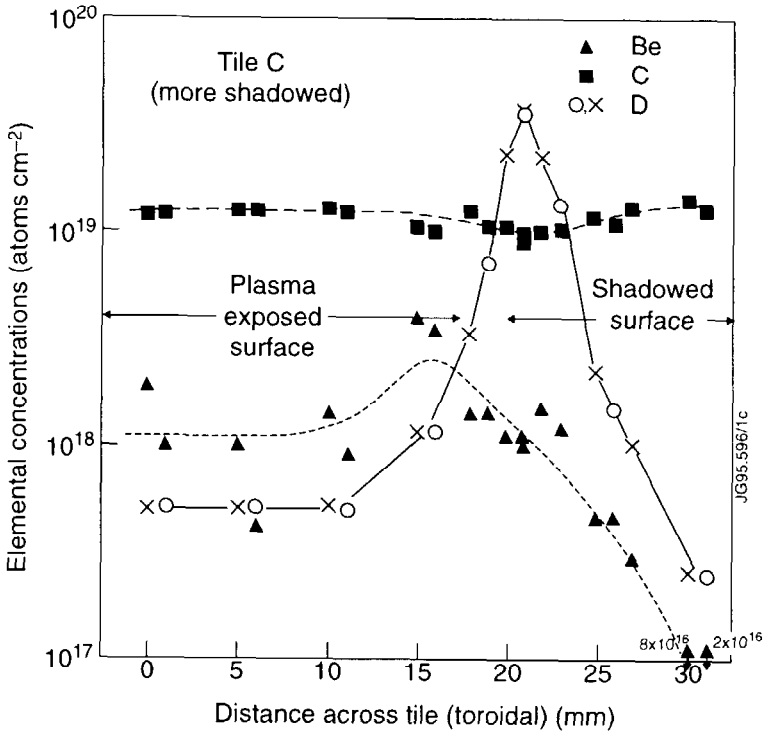

Fig.14: C, Be and D analyses by NRA recorded along two adjacent lines across (toroidally) tile 13A. (The analysis points from left to right across the figure correspond to points running from right to left across the tile as shown in Fig.12.)

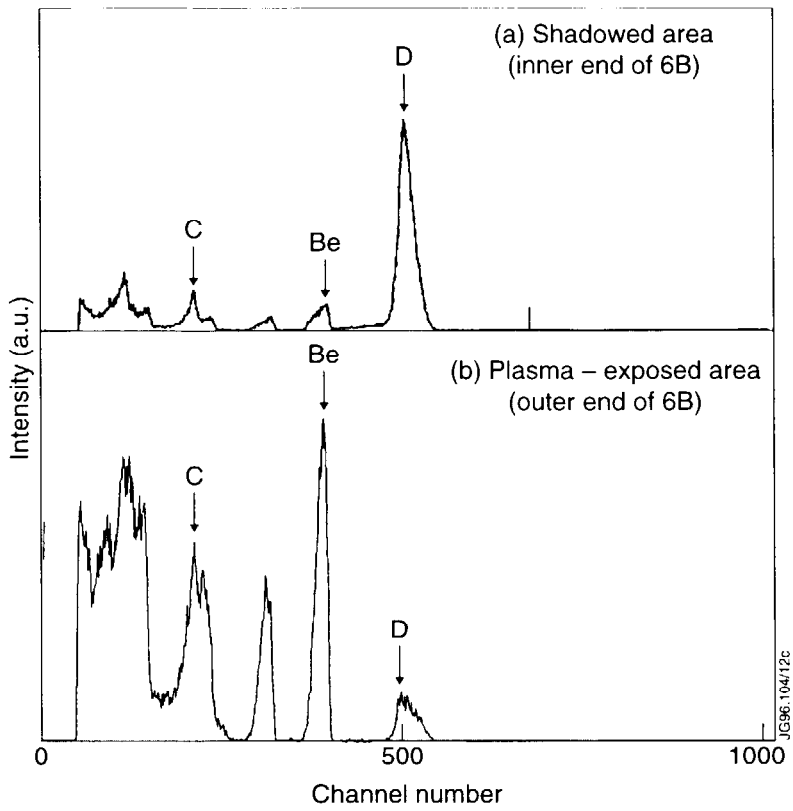

Fig.15: NRA spectra from two points on a beryllium tile exposed in position 6A to operations in 1995. The upper spectrum was recorded from within the shadowed region near the end of the tile deeper into the SOL, the lower spectrum from an area at the other end of the tile in the plasma-exposed region.

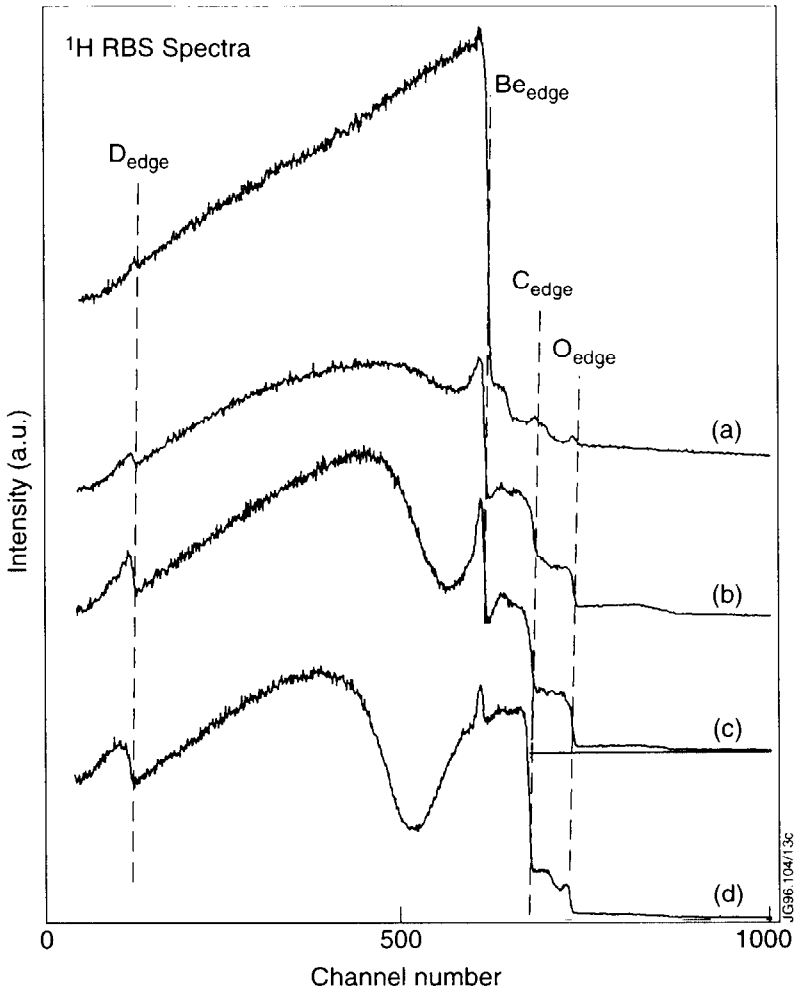

Fig.16: Proton RBS spectra from (a) the centre of the melt area on tile 12B, (b) the plasma-exposed area deep in the SOL on tile 5B, (c) the shadowed area on 6B close to the point from which the NRA spectrum of Fig.15(b) was recorded, (d) the area covered with a thick redeposited film on tile 5B.

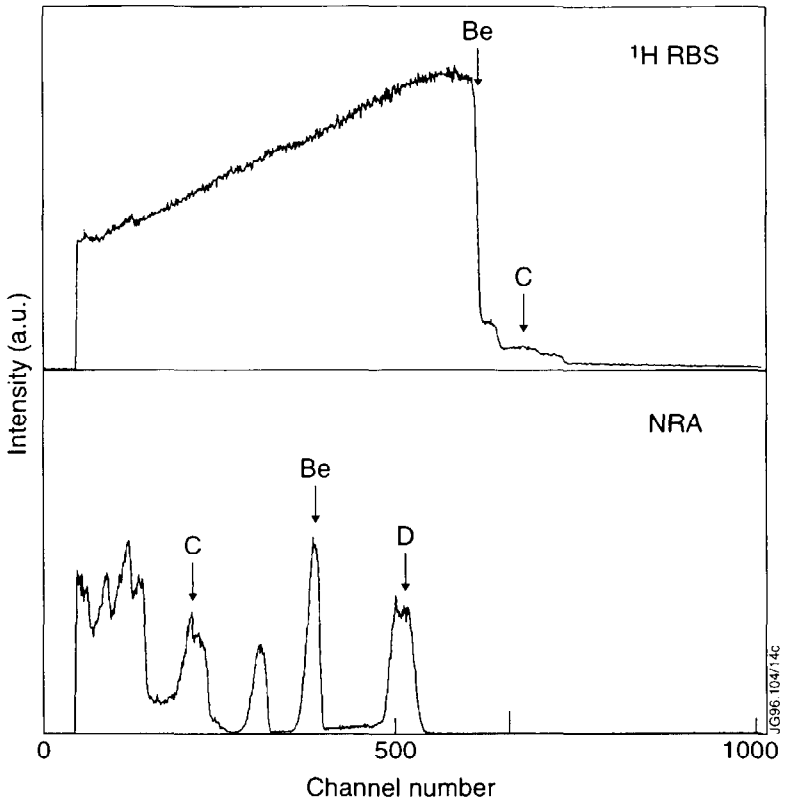

Fig.17: The NRA and proton RBS spectra from an area of tile 8A just outside the region which had been melted during plasma operations.

APPENDIX A

HYDROGEN ISOTOPE ANALYSIS OF THICK LAYERS DEPOSITED IN TOKAMAKS

J P Coad, B G Skorodumov*, V G Ulanov* and C H Wu**
JET Joint Undertaking, Abingdon, Oxon OX14 3EA, UK
*Institute of Nuclear Physics, Academy of Science of Uzbekistan, 702132 Tashkent, Uzbekistan
**The NET Team, Max-Planck-Institut fur Plasmaphysik, D-85748 Garching, Germany

ABSTRACT

Predictions can be made of the tritium retention in future tokamaks such as ITER based on analyses of the D retention in redeposited films in existing tokamaks. However, although amounts of H+D up to the saturation level are frequently observed, measurement is invariably by Ion Beam methods such as NRA and ERDA which only analyse to a depth of the order of a micron, whilst it is only the total content of very thick layers that is of relevance to ITER. This paper compares these near-surface data with methods developed to determine the composition throughout thick C-H films (~100 microns) such as Neutron-induced Elastic Recoil Detection Analysis (n-ERDA) and SIMS and Nuclear Microprobe analysis of specially prepared cross-sections.

1. INTRODUCTION

The primary mechanism for hydrogen retention in large tokamaks is codeposition with (and/or implantation into) material eroded from areas of plasma-facing components (PFC) with high incident fluxes and redeposited in regions of lower fluxes. If the PFCs are made of carbon in the form of graphite the saturation level of H-isotope trapping in redeposited layers at <270C has been shown to be given by H:C≅0.4:1 (1). In a long pulse, high power machine such as the planned **I**nternational **T**hermonuclear **E**xperimental **R**eactor (ITER) redeposited films up to millimetres in thickness may accumulate at the deposition-dominated wall areas. If the machine is fuelled by a 50% deuterium (D)/50% tritium (T) mixture, then T may be trapped at up to 0.2 times the amount of C in these thick layers, and retention of this magnitude would be unacceptable both from radioactivity and cost considerations.

In the post-mortem analysis of PFCs from JET and other tokamaks, similar amounts of H and D are generally observed in the near-surface region: since JET is normally fuelled with D the reason for the prevalence of H is unclear (2). However, as a result a saturation level of

H-isotopes in the near-surface region may correspond to an analysed retention of D of about 0.2 times the amount of C, and D at this level has frequently been observed in surveys of the PFCs in JET (3,4). Most of these measurements have been made using the **I**on **B**eam **A**nalysis (IBA) variant **N**uclear **R**eaction **A**nalysis (NRA), and with this technique usually only the outermost 1 micron (approximately) of the surface is analysed. Redeposited layers up to 130 microns thick have been measured in JET by sectioning the films on the flanks of the discrete limiters used until 1986 (5), and it is clearly important for the retained D inventory to know whether or not the D concentration throughout the film is the same as that seen by NRA in the outermost micron. A **S**econdary **I**on **M**ass **S**pectroscopy (SIMS) profile was made at a different point on the limiter where the film was 24 microns thick which showed that the D (and H) concentrations appeared to start high at the surface, but then fell by about an order of magnitude within the bulk of the film (5). However, the SIMS technique, which consists of sputtering material from a surface using an ion gun and analysing the ion content of the sputtered material entering a mass spectrometer, cannot be considered to be quantitative except in certain well-defined situations. Firstly the sputtering yield for an impurity element in a surface can vary over orders of magnitude depending on the surface roughness, the composition of the substrate and the binding configuration of the impurity. Secondly the fraction of material sputtered as ions and detected by the spectrometer varies by many orders of magnitude for different elements, and thirdly the composition profiles into the surface can be severely distorted due to differential sputtering, knock-on and shadowing effects.

Thus JET data (which give a similar picture for H-isotope retention to other tokamaks) generally show high surface (~1 micron) concentrations of retained H and D, and provide an example of lower concentrations into the bulk of a thick redeposited film. This paper describes the assessment of techniques for determining the H-isotope content of thick (>10 micron) films and their application to the analysis of the same thick redeposited films from the 1986 JET limiters.

2. EXPERIMENTAL RESULTS

(a) Preparation of samples

The ideal situation would be to be able to make an analysis in situ, or at least on a complete component after removal from the tokamak. However, since the limiter tiles removed from JET after the 1986 operations were each 450 x 120 x 77 mm, the only technique able to analyse a complete tile was IBA using a large target chamber specially constructed for analysing JET components. In order to investigate other methods it was therefore necessary to prepare smaller samples: samples were cut from the flanks of one of the limiter tiles as shown in Figure 1. Samples cut from the same part of the profile of the tile (eg samples 3, 8 and 11)

are assumed to be equivalent. Since the films are very thick, it is possible to profile through the film by analysing a cross-section of the film, if the spatial resolution of the technique is good enough, and this can be enhanced by producing a taper section which improves the resolution by up to an order of magnitude by increasing the apparent thickness of the film. Thus it can be seen that sections were prepared from samples cut adjacent to the conventional coupons. However it should be noted that preparation of sections may affect the results subsequently obtained by smearing material across the surface or leaching out certain components by reaction with the potting resin or polishing solution. (A possible method of preparing a section through a thick film without metallographic polishing is ion beam slope cutting (6,7). The area to be analysed is the side wall of a crater formed by ion bombardment, the line of the wall being defined by a sharp-edged screen. However development of the technique from films a few microns thick (7) to films of the order of 100 microns has yet to be demonstrated.)

(b) NRA analyses of tile samples and an implanted standard

The samples cut from the JET limiter tile were analysed by NRA to obtain the surface (~1 micron) concentration of D using the $D(^3He,p)^4He$ reaction. The results are given in the first column of Table 1. To check the quantification some graphite samples were also implanted to saturation with 5 keV deuterons over a 5 mm diameter region, which according to TRIM calculations should provide a surface containing 6.10^{17} deuterium atoms cm^{-2} within the outermost 0.15 microns. One of these standards analysed by NRA and by other techniques is included in Table 1 and the NRA result (which was duplicated in different laboratories) is shown to be in good agreement with the calculations.

(c) Heavy Ion Induced Elastic Recoil Detection Analysis

Another of the IBA family is **E**lastic **R**ecoil **D**etection **A**nalysis (ERDA) wherein an ion beam is incident at glancing angle and atoms may be ejected from the surface after an elastic collision with the incident ion (that is, most of the incident energy is transferred to a recoil in the collision). The detector for the ejected particles is placed at glancing angle in the forward direction. In the most common form of this technique a helium ion beam is employed at energies up to 3 MeV. Each of the H isotopes can be separately analysed by this method, and the depth of analysis is about 1 micron. The technique is much more dependent on surface roughness than NRA, but is usually the only way to obtain an idea of the H (ie protium) surface concentration. However, if very much higher incident energies are employed the analysable depth increases, and if ions of a heavier element are used the range of masses detected is also increased: this is the technique known as Heavy Ion ERDA (8,9). Ejected ions are detected using ionisation chambers wherein an ion from the sample passes through the

chambers in series. The maximum value of the energy loss dE/dx, i.e. the Bragg peak height, of the detected particles in the detector gas depends on their atomic charge number Z. By suitable adjustment of the detectors, the atomic number and energy of each ion can be measured simultaneously. From the number of ions detected as a function of energy, for each element in the energy loss versus energy plots, can be calculated the depth distribution of that element into the surface.

Figure 2 shows depth distributions for the masses 1, 2, 12 and 16 (H, D, C and O, respectively) through the outermost 2 microns of the surface of sample 8 from the 1986 JET limiter tile. Profiles can be derived to about 10 microns for the H isotopes under these Heavy Ion ERDA conditions, but it can be seen in Fig. 2 that the H, D and O are mostly restricted to the outermost $^1/_2$ micron of the surface. Note, however, that the H continues at ~20% of its peak value beyond 2 microns, whereas the D concentration falls to zero. Integrating under the D depth profile and using a surface density for graphite of 10^{19} atoms cm^{-2} gives a concentration of 3.10^{17} D atoms cm^{-2} on sample 8. As seen in Table 1 this is lower than the NRA value, but factors of two between these methods have been seen previously (10) and may be due to a difference in the calibration of the Heavy Ion ERDA technique.

(d) Neutron-induced Elastic Recoil Detection Analysis (n-ERDA)

ERDA with primary ions can be seen from the previous section to be potentially very powerful, but the depth attainable is limited by the need to use glancing angles (to approach the forward scattering conditions necessary for maximum momentum conservation, and which also imposes severe practical limitations on the sample) and by the penetration of the primary beam. These limitations are eased if **neutrons** incident on the rear of the sample are the primary source. Fast neutrons will pass through samples a few millimetres thick without significant energy loss or attenuation, and the maximum escape depth for the recoil particles (i.e. normal to the surface) can be utilised (11). For graphite samples total H isotope concentrations can be absolutely determined from comparison with $TiH_{1.87}$ and $TiD_{1.97}$ standard samples for films 300 - 400 microns thick using 14 MeV neutrons, with variations in concentration with depth visible with a resolution for D analysis of ~30 microns: using 2.5 MeV neutrons these figures become ~50 and ~5 microns, respectively. In these experiments a 14 MeV neutron source was employed, and a three detector telescope using silicon sensors was used to simultaneously measure energy loss and energy for each particle. One disadvantage of the method is that the neutron flux at the sample obtainable from an accelerator used as a neutron generator is much lower than the ion flux that can be achieved, so counting times are much longer (typically ~ an hour) for reasonable statistics and the absolute sensitivity of the technique is also lower than for the ion beam techniques.

The total amounts of H and D present throughout the thickness of the films (since they are well within the detection range for 14 MeV neutrons) are listed in the right-hand columns of Table 1. It can be seen that according to n-ERDA the total amounts of D in films up to 120 microns thick are not much greater than those detected in the outermost micron by NRA, although there was good agreement in the analysis of the D standard. n-ERDA also showed larger quantities of H than D in the films. In order to shed light on these somewhat surprising results, the data were deconvoluted to provide depth profiles through the thickest film (sample 4), and these experimental profiles were compared with profiles simulated by Monte Carlo methods for a number of distribution scenarios. The results for D are shown in Figure 3. It can be seen in the figure that the data are a good match to a distribution with 33% of the D at the surface and the remainder tailing in approximately 70 microns into the film, but clearly do not match the other model distributions in the figure. Likewise Figure 4 shows the experimental profile for H, and in this case there is a good match with a distribution with a constant level for 70 microns from the surface followed by a concentration decreasing from half that value to zero over the next 50 microns.

The distributions in Figs 3 and 4 are merely indicative and in reality there may be a wealth of fine structure, since the inherent resolution of the n-ERDA technique is rather poor. However, uniform concentrations of either H or D throughout the film are precluded, and there is a genuine difference between the distributions of the two isotopes: much more detailed information on the distribution in the outer part of the film would be obtained using 2.5 MeV neutrons. Assuming the best-fit profiles to be correct, the H and D contents of the outermost 1 micron would be 1.10^{17} and 2.7×10^{17} atoms cm^{-2}, respectively.

Thus the n-ERDA data suggest the D is concentrated at the surface, and are not inconsistent with the NRA results, although the expected amount in the outermost micron is about half the NRA amount (as was the Heavy Ion ERDA result). Note also that the H content of the outermost micron is ~ one-third of the D content (as indeed was shown by Heavy Ion ERDA on the adjacent sample), so that a more surface specific technique would suggest there is **more** D than H in the film whereas in fact there is almost an order of magnitude **less**.

(e) Nuclear Microprobe analysis of sections

The Nuclear Microprobe produces a focussed ion beam with a minimum diameter of about 5 microns. Thus in principle it is possible to produce NRA profiles through a thick film with a resolution of about 5 microns by analysing a section through the film in a Nuclear Microprobe. Indeed, this resolution can be improved to about 1 micron by producing a taper section through the film. At the maximum resolution the beam current becomes too low for analysis in a reasonable time, but since the film extends uniformly in one direction (supposedly) the beam can be extended parallel to the film surface without degrading depth

resolution. In this investigation the bombarded area was thus oblong, 15 microns wide (which is thus the resolution across the section) and 100 microns long, allowing good statistics in about 60 secs. Figure 5 shows a plot of D peak intensity (in arbitrary units) versus distance across the redeposited film section. This section was a taper section of a 60 micron thick film polished at 5 degrees to the surface of the sample: the film appears 240 microns across, so the tapering improves resolution by a factor of 4. (The factor of 11 that might be expected geometrically does not appear to be realised). The sample was taken from a different part of the 1986 limiter, though from a similar section of tile to that shown in Fig.1.

The Nuclear Microprobe analysis shows a peak of D at the surface, the width of which is approximately equal to the beam width, so the actual width of the D-rich layer in this taper section must be <<15 microns, and therefore in normal section must be of the order of a micron or less. Integrating under the surface peak and under the rest of the depth distribution suggests about half of the D is in the surface peak, a result similar to the n-ERDA analysis of another area of film.

(f) SIMS profiling and analysis of sections

As mentioned in the Introduction, a SIMS analysis of a similar limiter tile from 1986 showed lower H and D levels within than at the surface (5), but there are many possible errors associated with the measurement. However, many of the errors associated with sputter profiling disappear if SIMS is used to image the cross-section, as signal intensities from all points in the section should be directly comparable. Furthermore since the primary ion beam used can be focussed to << 1 micron the potential resolution makes the technique complementary to the Nuclear Microprobe. A number of sections, including sample 12, from limiter tiles were examined by SIMS, but the results were disappointing. When the whole cross-section was viewed good secondary electron images were obtained, and ions of impurity elements such as Cr and Ni could be mapped. However the D and H distributions were distorted and could not be used to compare the quantities of each isotope across the film. It was possible to see that there was generally an aggregation of H and D at the surface, and occasionally accumulations at defects within the film or at the film/substrate interface. It was also clear that on the micron scale the composition parallel to the surface, as well as through the film, was variable.

Conventional SIMS was performed (i.e. by bombarding the the outer surface) on samples 1 - 5 and the D standard. Figure 6 shows the signal intensities in the mass peaks 1, 2 and 12 (H, D and C, respectively) versus bombardment time for the D standard. The maximum D signal level is about a factor of 7 lower than the C signal, so this should correspond to the saturation ratio for D:C of 0.4:1 (1). The D level falls off after ~300 secs, which according to TRIM code predictions should correspond to a depth of ~150 nm. Figure 7

shows a similar spectrum recorded from the tile sample 4. Again the maximum D signal is about a factor of 7 lower than the C signal, so since the matrix is again essentially carbon, this should also indicate the saturation level for D in C. Note, however, that this is only for <100 secs at the start of the profiling. The beam current density was about twice that used in Fig. 6 (hence the C signal is 10^4 rather than 4.10^3) so the amount sputtered away in this time (again assuming similar behaviour to the standard) is ~100 nm. The D concentration then stabilises at about a factor of 5 less than its earlier value.

The steps up and down in signal levels seen in Fig. 7 after ~600 and ~1000 secs are due to deliberately raising the beam current density by a factor of two and then returning it to the initial value. The signals from elements present in the substrate should also double, but impurities originating from the vacuum system should not respond in this manner. In particular H is always present in the system. From the behaviour of the H signal in Fig. 7 it can be seen that about half of the H at that time is really part of the film whilst the rest may be contamination. By comparison with Fig. 7 and profiles from other samples analysed at that time, it seems probable that most if not all of the H seen in Fig. 6 comes from contamination. It should be noted that the relative intensities of the H and D signals cannot be taken as a measure of their relative quantities in the film, since the ion sputtering characteristics and detection efficiencies may differ.

3. DISCUSSION

All the analyses of these redeposited films on samples cut from the flank of one of the discrete limiters used in JET in 1986 agree that the D is peaked within the outermost micron (approximately) of the film, and that there is perhaps a similar amount in total in the remaining thickness of the film. Thus there is no serious discrepancy between any one technique and others. None of the techniques offers a non-destructive method of analysing the large components likely to be used as PFCs in ITER, and these data highlight the problem that **surface** analysis by NRA (which can be done non-destructively) cannot be used to predict **bulk** composition.

n-ERDA can provide a quantitative analysis simultaneously for each of the isotopes H, D and T through films up to some hundreds of microns thick (and would give the ratios H:D:T in the outer part of films in the millimetre range, should they occur). The method does rely on neutrons penetrating through the sample without significant losses, but the resulting limitations on sample composition and thickness have not been fully assessed. Samples of graphite a few millimetres thick as in this work present no problem, so it may be possible to analyse through certain first wall components, or to arrange for special components with the outer few millimetres detachable in areas where rapid film growth is expected. If samples have to be cut out for analysis, then cutting out samples to a rough thickness tolerance is all

that is required for n-ERDA as well as the surface layer examination techniques like Heavy Ion ERDA and SIMS, whilst that is only the first step in the preparation of the sections necessary for Nuclear Microprobe analysis. There is also a risk that the polishing process may introduce anomalies into the film analysis, though there was no evidence of such problems in this investigation: ion beam slope cutting (6,7) may offer an alternative preparation method. Smearing effects during sectioning would, however, be expected to be too great to allow second order measurements such as bulk diffusion to be made using either technique. The Nuclear Microprobe could also measure T depth profiles for films deposited from D-T plasmas by using a different NRA reaction, but, like n-ERDA, does not have the sensitivity to measure the T in films deposited from D-D plasmas. Measurement of H by ERDA is also possible in principle, but would be very difficult in practice due to the glancing angle geometry required.

The samples used in this work are the only known examples of very thick (~100 microns or more) material redeposited in a tokamak, and it was hoped that they would contain significant D levels throughout the film to provide a better test for the analysis options. The fact that the SIMS analysis previously carried out on the tiles (5) showed reduced H and D levels within the film means that the localisation of the D to the surface in these analyses several years later is unlikely to have occurred merely with time. The discrete limiters regularly reached temperatures in excess of 1000C at the erosion zones to either side of the centre of the tile during plasma pulses, and temperatures in the redeposition zone must also have regularly exceeded the 400C at which the film starts to degas (12): a number of the plasma pulses also terminated in disruptions which can cause large transient heat loads. Thus thermal outgassing of the samples seems a plausible reason for the low total D content of these films, and it may be possible for high D levels to exist throughout a thick film provided the temperature is always kept low enough.

4. CONCLUSIONS

The H, D and T contents of films up to hundreds of microns thick can be simultaneously measured quantitatively by n-ERDA. For thick film analysis a source of 14 MeV neutrons is required, whilst better resolution in depth distributions is obtained using 2.5 MeV neutrons. It is intended to develop a n-ERDA analysis facility capable of providing both energies in the near future.

Metallographic sectioning can also be used to provide D depth profiles through thick films with the Nuclear Microprobe. These tests show that the depth resolution obtainable is a few microns using taper sections, which is equivalent to about 1 micron in a normal section through the film. Of course considerable effort is required to produce the sections, but the

polishing process does not appear to have a deleterious effect on the profiles. T depth profiles could also be measured for films deposited from D-T plasmas.

These thick (up to 130 micron) redeposited films had a total D content no larger than thin films found elsewhere in JET, and the D concentration within the surface was at least an order of magnitude less than in the outermost 1 micron. It is believed that this is due to thermal outgassing of the films when the limiters were heated to ~1000C by the JET plasma during high power discharges and/or as the result of disruptions.

5. ACKNOWLEDGEMENTS

The help of Dr R Behrisch (Max-Planck Institut fur Plasmaphysik, Garching) and Dr W Assmann and H Huber (Ludwig Maximilians Universitaet Muenchen) with Heavy Ion ERDA analysis, Dr S Sugden (AEA Technology) and Dr A Clough (Surrey University) with Nuclear Microprobe analysis, B Farmery (Sussex University) with NRA analysis and Dr A Chew (Loughborough Consultants) with SIMS analysis is gratefully acknowledged. This work was supported by NET in the context of the European Home Team contribution to ITER (ITER Task T62 of the 1994 Comprehensive Task Agreement).

6. REFERENCES

(1) K L Wilson and W L Hsu, J Nucl. Materials, **145-147** (1987) 121

(2) J P Coad, J Nucl. Materials, to be published.

(3) H Bergsaker, R Behrisch, J P Coad, J Ehrenberg, B Emmoth, S K Erents, G M McCracken, A P Martinelli and J W Partridge, J Nucl. Materials, **145-147** (1987) 727.

(4) J P Coad, R Behrisch, H Bergsaker, J Ehrenberg, B Emmoth, J Partridge, G Saibene, R Sartori, J C B Simpson and Wen-Min Wang, J Nucl. Materials, **162-164** (1989) 533

(5) G M McCracken, D H J Goodall, P C Stangeby, J P Coad, J Roth, B Denne and R Behrisch, ibid, p356.

(6) W Hauffe, Beitr. Elektronenmikr. Direktabb. Oberfl., **23** (1990) 305.

(7) D Grambole, F Herrmann, R Klabes, W Hauffe and R Behrisch, Nucl. Instr. and Methods, **B68** (1992) 154.

(8) R Behrisch, R Grotzschel, E Hentschel and W Assmann, ibid, p245

(9) U Kreissig, R Grotzschel and R Behrisch, Nucl. Instr. and Methods, **B85** (1994) 71

(10) R Behrisch, A P Martinelli, S Grigull, R Grotzschel, U Kreissig, D Hildebrandt and W Schneider, J Nucl. Materials **220-222** (1995) 590

(11) B G Skorodumov, I O Yatsevitch, V G Ulanov, E V Zhukovska and O A Zhukovsky, Nucl. Instr. and Methods, **B85** (1994) 803

(12) R A Causey, W R Wampler and D Walsh, J Nucl. Materials, **176&177** (1990) 987

TABLE 1 Comparison of the analyses (all in units of 10^{17} atoms cm^{-2}) of H-isotopes in carbon samples by different techniques.

	NRA	HIERD	NERD			
Sample Number			Outer Micron		Total in Film	
			H	D	H	D
1 or 6	4.7					
2 or 7	5.4				19.0	6.2
3 or 8	5.0	3.0			72.0	8.0
4 or 9	4.8		1.0	2.7	65.0	8.5
5 or 10	2.6				87.0	5.3
D-standard 2	5.1 (5.3)				b/g	7.5

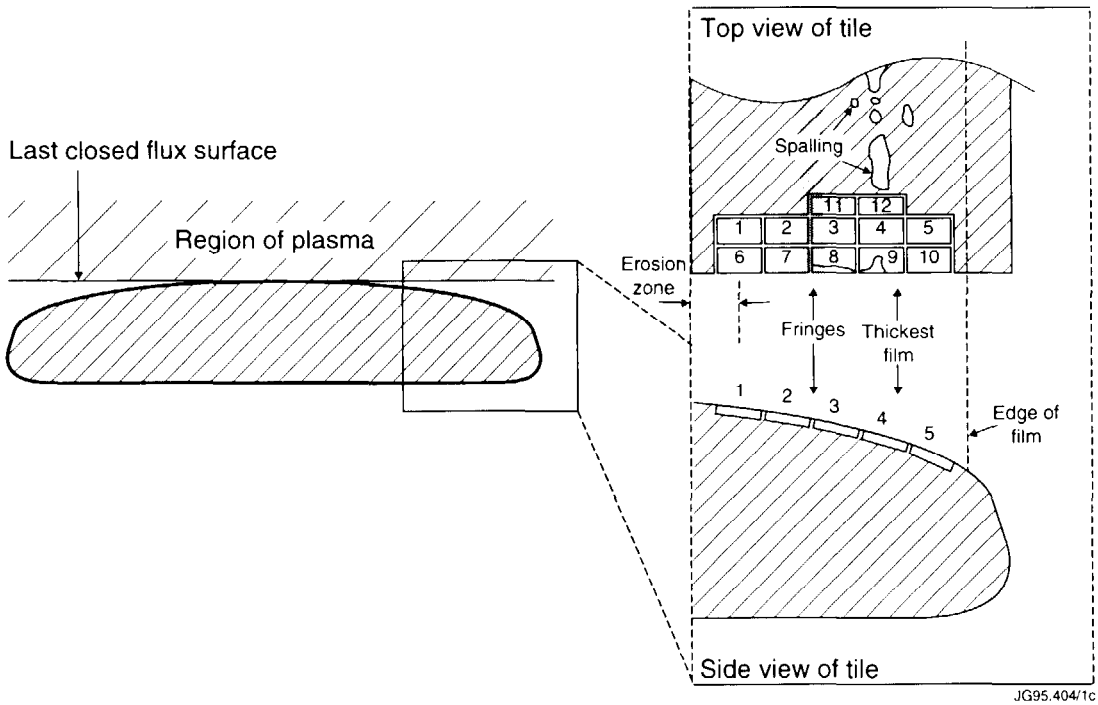

Fig.1: A diagram showing the original locations of the samples cut from a JET limiter tile used in this study, and the position of the tile relative to the JET plasma.

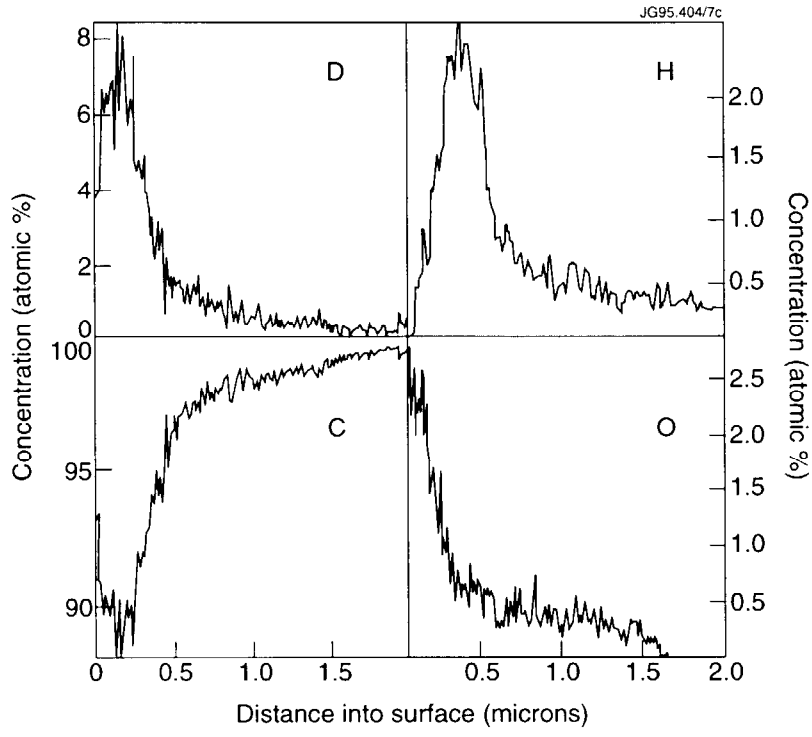

Fig.2: Depth distributions for masses 1, 2, 12 and 16 (H, D, C and O, respectively) determined by Heavy Ion ERDA in sample 8.

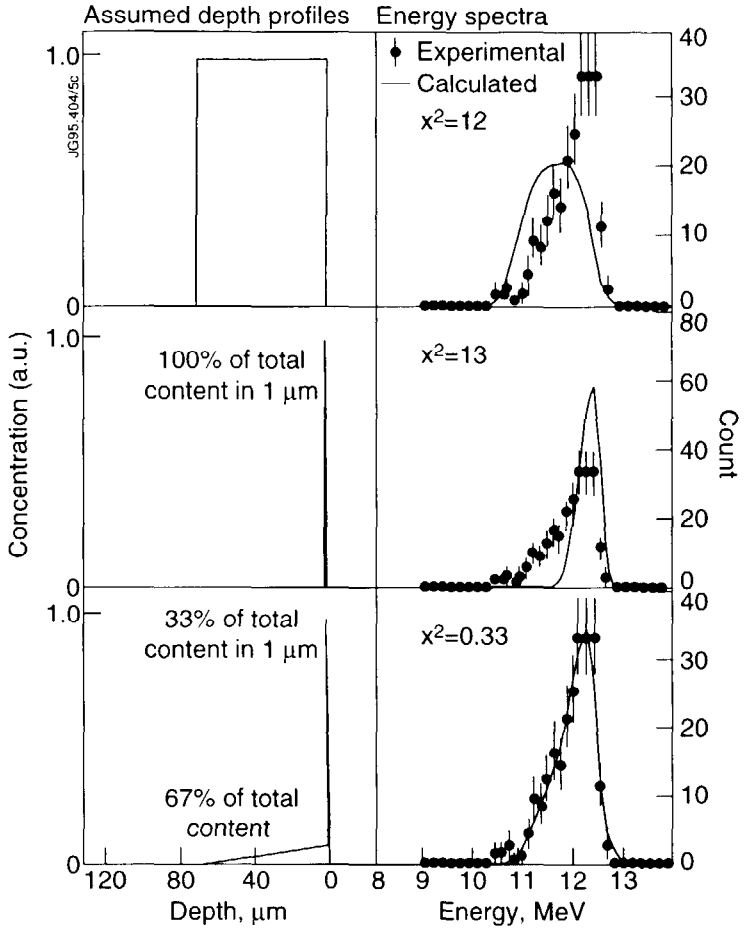

Fig.3: The n-ERDA spectrum for D from sample 4 compared with the calculated spectrum expected for each of three different D depth distributions in the film.

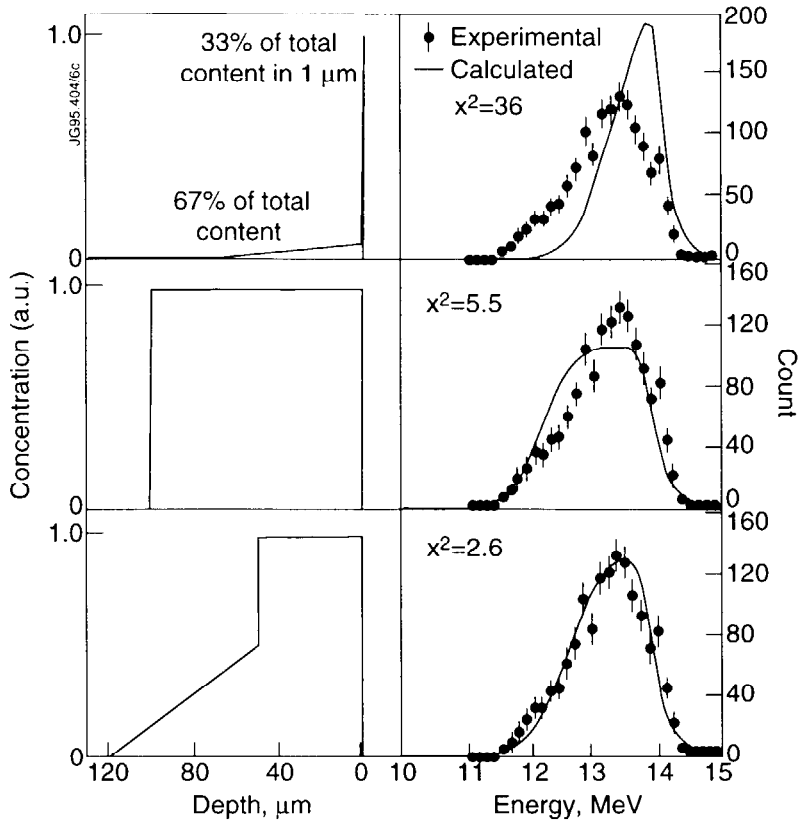

Fig.4: The n-ERDA spectrum for H from sample 4 compared with the calculated spectrum expected for each of three different H depth distributions in the film.

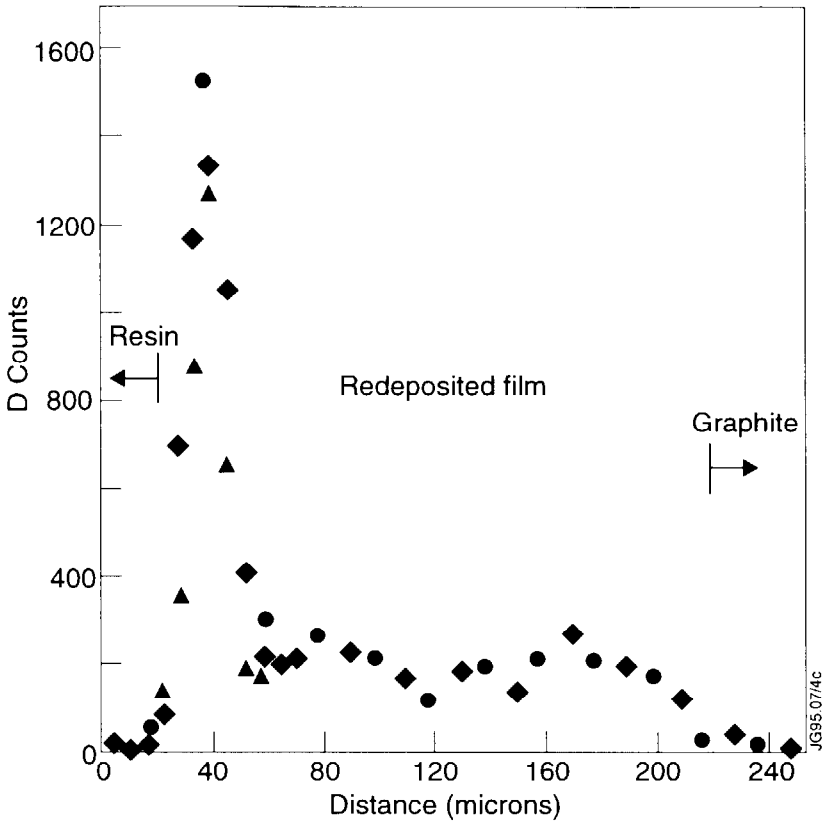

Fig.5: The D peak intensity versus distance across the taper section of a redeposited film obtained by NRA using a Nuclear Microprobe.

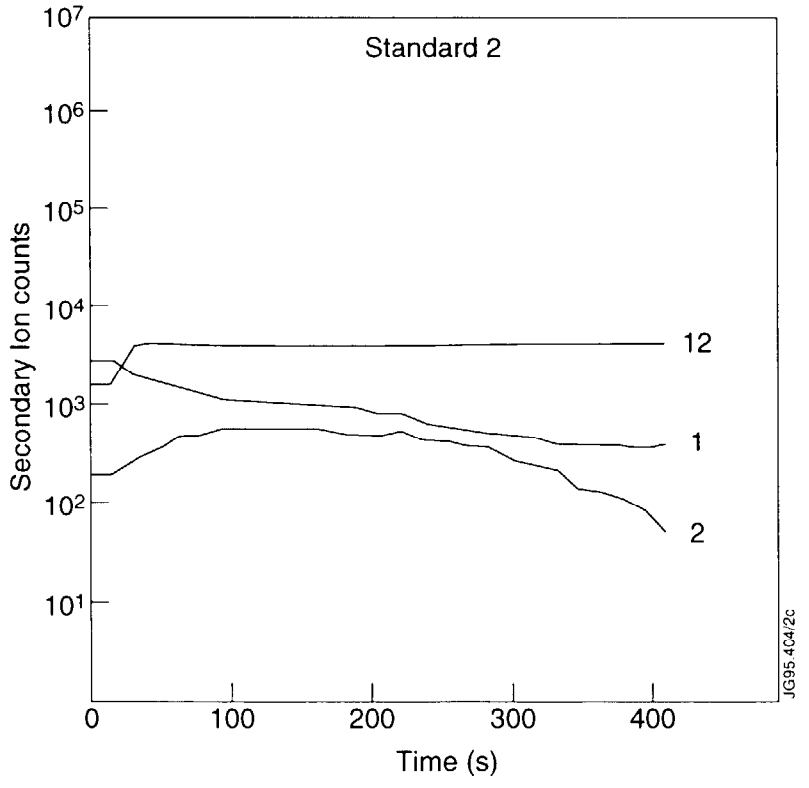

Fig.6: Signal intensities for masses 1, 2 and 12 (H, D and C, respectively) versus sputtering time (i.e. depth) into a D-implanted graphite standard.

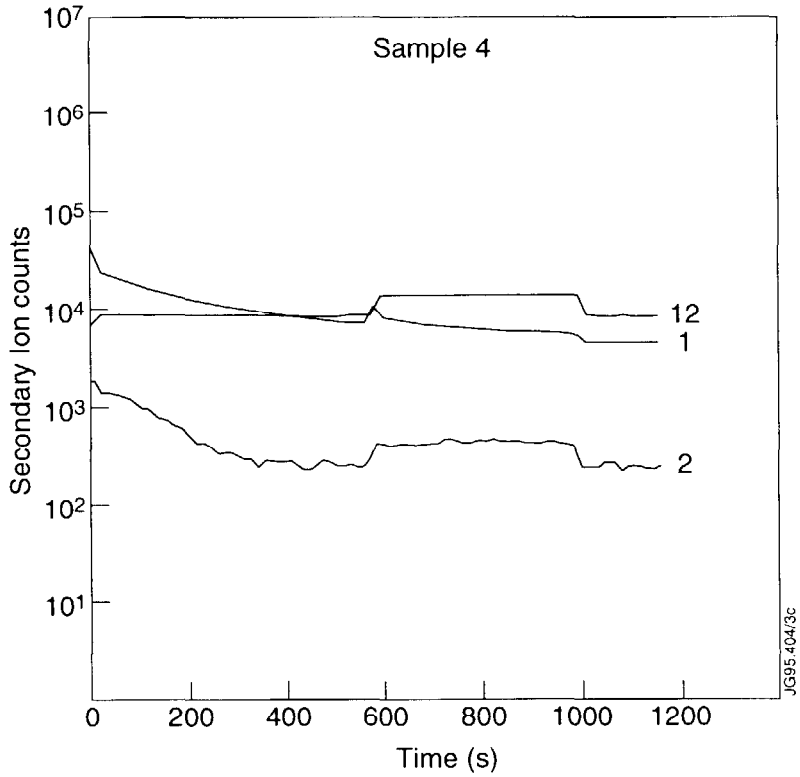

Fig.7: Signal intensities for masses 1, 2 and 12 (H, D and C, respectively) versus sputtering time (i.e. depth) into sample 4.

Figure Captions

Figure 1: A radial cross-section of the JET Mark I divertor which was in use during 1994 and 1995.

Figure 2: A drawing of a section of the JET Mark I divertor.

Figure 3: A schematic toroidal cross-section of some divertor tiles to show the shadowing of part of each tile by its neighbour.

Figure 5: Differential cross-section for the ^{3}He (d,p)^{4}He reaction as measured by different authors.

Figure 6: Excitation curves for protons from ^{12}C (^{3}He,p)^{14}N corresponding to formation of ^{14}N in its ground state and first two excited states.

Figure 7: NRA spectra from a D-implanted graphite standard using three different ^{3}He primary ion beam energies.

Figure 8: An NRA spectrum recorded with a 2.5 MeV ^{3}He ion beam from a Be divertor tile exposed in JET in 1995 (central part of figure), with an expansion of the D peak (top part) and a reconstructed depth distribution using the data of Fig. 6 and the stopping power for ^{3}He ions.

Figure 9: ^{4}He RBS spectra from a relatively clean area of the graphite divertor tiles (upper part), and from a tile showing heavy redeposition from the plasma (lower part).

Figure 10: An RBS spectrum recorded using a proton beam from the same area as analysed in the lower part of Fig.9.

Figure 11: A PIXE spectrum recorded from the same area as the RBS spectrum of Fig. 10 and simultaneously using the same proton beam.

Figure 12: An overall view of the D distribution on the divertor floor tiles removed from the torus in September 1994 (for the outer half of the divertor), the D analyses being in units of 10^{17} atoms cm^{-2}.

Figure 13: An overall view of the D distribution on the divertor floor tiles removed from the torus in September 1994 (the innermost two tiles), the D analyses being in units of 10^{17} atoms cm^{-2}.

Figure 14: C, Be and D analyses by NRA recorded along two adjacent lines across (toroidally) tile 13A. (The analysis points from left to right across the figure correspond to points running from right to left across the tile as shown in Fig.12.)

Figure 15: NRA spectra from two points on a beryllium tile exposed in position 6A to operations in 1995. The upper spectrum was recorded from within the shadowed region near the end of the tile deeper into the SOL, the lower spectrum from an area at the other end of the tile in the plasma-exposed region

Figure 16: Proton RBS spectra from (a) the centre of the melt area on tile 12B, (b) the plasma-exposed area deep in the SOL on tile 5B, (c) the shadowed area on 6B close to the point from which the NRA spectrum of Fig. 15(b) was recorded, (d) the area covered with a thick redeposited film on tile 5B.

Figure 17: The NRA and proton RBS spectra from an area of tile 8A just outside the region which had been melted during plasma operations.